Volume 4, Issue 4, 2015, 321-334 **ISSN 2284-6808**

Letters in Applied NanoBioScience

www.NanoBioLetters.com

Review Article **Open Access Journal**

Received: 25.08.2015 / Revised: 30.09.2015 / Accepted: 25.11.2015 / Published on-line: 30.11.2015

Atomic Force Microscopy: an innovative technology to explore cardiomyocyte cell surface in cardiac physio/pathophysiology

Véronique Lachaize [1,2,3,4], Cécile Formosa [2,3], Georgiy Smolyakov [1], Céline Guilbeau-Frugier [4,5,6], Céline Galés [2,4], Etienne Dague [1,2,3]

[1] CNRS, ITAV-USR3505 ; F-31100 Toulouse, France
[2] CNRS, LAAS, 7 avenue du colonel Roche, F-31400 Toulouse, France
[3] Université de Toulouse, UPS, ITAV, LAAS, F-31000 Toulouse, France
[4] Institut des Maladies Métaboliques et Cardiovasculaires, INSERM UMR 1048, Toulouse, France
[5] INSERM Department of Histopathology, Centre Hospitalier Universitaire de Toulouse, 31432 Toulouse, France
[6] Centre de Microscopie Électronique Appliquée à la Biologie, Faculté de Médecine Rangueil, 31062 Toulouse, France

*corresponding author e-mail address: ***edague@laas.fr***

ABSTRACT

Atomic Force Microscopy (AFM) has emerged these recent years as a multifunctional toolbox for studying biological samples in physiological conditions. Although its use has spread among biologists community, cardiology remains a scientific field where AFM has not been extensively used yet. Heart diseases are nowadays a major human threat, and cause the death of millions of people each year. A convergent point to all heart diseases seems to be related to the defect of the cardiomyocyte, the contractile unit of the heart. For this reason, many scientists got interested in this cell type. However, very few studies use a technology such as AFM and its derivatives (force spectroscopy, multiparametric imaging) to explore this cell. The aim of this review is thus to give a comprehensive analysis of the interest of the biophysical approach made possible by AFM studies. We will show how AFM has been and can be used to study fixed or living cardiomyocytes, and, how combined with other types of microscopy, it can help getting a better understanding of the effects of pathologies or drugs. This review is the first dedicated to the use of AFM technics in cardiology, and gives new insights into the fundamental questions surrounding cardiomyocytes, that can be answered using such a technology.

Keywords: *Atomic Force Microscopy, Imaging, Force Spectroscopy, Heart diseases, Cardiomyocyte.*

1. INTRODUCTION

Cardiovascular diseases are a major health issue, and cause each year the death of 17.5 million people worldwide, with no distinction between men and women. Among these deaths, 8.5 million originate from heart diseases (Figure 1) [1] and statistics indicate that Heart Failure (HF) has a prevalence of over 23 million worldwide [2]. HF is a clinical syndrome characterized by the impairment of the contractile function of the heart occurring as a consequence of cardiac injuries. It is the convergent evolution of many heart diseases such as coronary diseases or myocardial infarction (MI) [3]. Although significant therapeutic options are now available for HF management, HF still remains the leading cause of morbidity and mortality in industrialized countries, and the number of patients suffering from HF increases over time. Indeed, many of the pharmacological therapies efficiently slow down the progression of HF, but do not stop it, suggesting that there is still an incomplete understanding of the molecular basis underlying the onset of HF. Thus, there is an urgent need for new treatment strategies that would improve the clinical outcomes of HF; but for that, identifying novel targets is mandatory.

Progression towards HF is a two steps process. The first step, called the compensation step, relies on the adaptative response of the heart to maintain a physiological cardiac output. It is characterized by the progressive hypertrophy of the heart muscle related to the increase in size of the contractile cells, cardiomyocytes (CM), which ultimately evolves towards the second step, called the decompensation step. During this second step, CMs death leads to the loss of the heart function and to the onset of HF [4]. Nowadays, pharmacological therapies recommended for HF management target essentially the events taking place during the compensation step and only delay the progression towards the decompensation step. Indeed, the molecular mechanisms responsible for the transition of the heart from the compensatory to the decompensatory step are still unknown. However, histological observations indicate that changes in CMs morphology (wavy CMs) but also CMs necrosis are key features of the decompensation step in human patients with end-stage HF [5]. Necrosis is a mechanism of cell death characterized by the rupture of the cell plasma membrane and the liberation of the cell content in the surrounding tissues that leads to an inflammatory reaction [6]. It thus follows that defects of the CM plasma membrane could participate to the onset of HF. However, this aspect was never thoroughly explored, most probably because of the lack of techniques that would allow the accurate exploration of the CM plasma membrane.

In this review, we will first present an overview of the structure/function of the CM. Then we will discuss on the different microscopic approaches that were used to study this cell. A next part of the review will be dedicated to the use of Atomic Force Microscopy (AFM) to study the CM plasma membrane and finally we will present the interest of such technology to unravel CMs structure and function in physio- and pathophysiological condition.

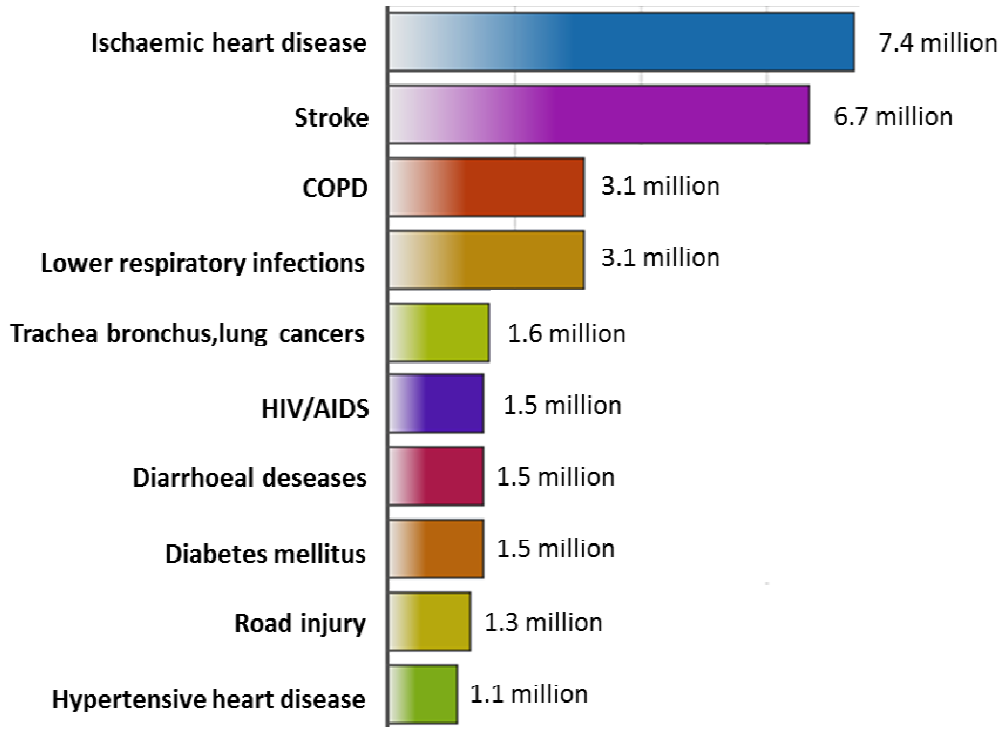

Figure 1. The 10 leading causes of death in the world (2012), A total of about 8.5 millions death is caused by cardiac diseases. Reprinted from WHOFact-sheet n°310.

2. STRUCTURE AND FUNCTION OF THE CARDIOMYOCYTE

The adult CM is a highly differentiated cell characterized by a typical "rod shape" (Figure 2A). CMs are relatively large cells with conserved size in all animal species ranging from 100-150 µm in length and 10-20 µm in width [7], but this size is an average and eg cardiomyocyte isolated from left ventricle, 2 months old mouse, were described to be 66±8.9 µm in length [7]. Actually CMs size depends on their location in the heart, (ie CMs form right ventricle are longer than CMs from left ventricle [7]). However, before becoming a highly differentiated and structured cell, the CM morphology evolves through a long postnatal maturation process [7]. Indeed, during embryonic development, the heart is subjected to low blood pressure, which dramatically increases at birth due to the onset of the pulmonary respiration. During this postnatal period allowing the heart growth (Figure 2B), the cardiac tissue architecture undergoes deep changes allowing the heart to adapt to its new hemodynamic conditions. At the cellular level, postnatal growth of the rodent heart begins with a first phase of hyperplasia (~until postnatal day 5) characterized by the proliferation of neonatal CMs. This first phase is then followed by a second phase of hypertrophy (from postnatal day 5 to 20) during which CMs stop their proliferation but increase their cellular mass (Figure 2B). From a morphological view, the maturation of the CM involves the differentiation of an immature neonatal contractile cell with a fibroblastic-like morphology into a mature adult cell characterized by a rod shape (Figure 2B). From a structural point of view, the adult mature CM is composed of (Figure 2A):

* The lateral membrane (LM, or sarcolemma) which plays a key role in connecting the extracellular matrix (ECM) to the intracellular contractile machinery and guarantees the 3D organization of the cardiac tissue. In addition, the LM of adult CMs is characterized by the presence of multiple intracellular tubular invaginations called T-Tubules (Transverse Tubules) making an intricate network around the myofibrils. T-Tubules structures are responsible for the excitation-contraction coupling of the CM, as well as for the in-depth transmission of the action potential allowing a homogeneous contraction across the CM.
* The Intercalated Disc (ID), localized at the longitudinal end of CMs and allowing them to directly and tightly interact with each other's. These direct interconnections between CMs ensure the synchronization of contraction between two adjacent CMs.
* The myofibrils play an important role in the architecture and function of CMs as they provide its basic contractile activity. Myofibrils also contribute to the spatial organization of other cytoplasmic components such as the interfibrillar mitochondria (IFM) providing the energy supply necessary for the contraction of CMs. Each myofibril is divided in several contractile units called sarcomeres, composed of actin and myosin filaments and delimited by two Z lines.

Examination of CM morphology is classically used in human pathology to detect anomalies in the cardiac tissue, and therefore to diagnose heart diseases [8]. For example, in HF, CMs undergo deep morphological changes, such as hypertrophy during the compensatory step and nuclei rounding or loss of the plasma membrane integrity promoted by necrosis programming during the

decompensation step [5]. Thus, the microscopy field including classical microscopy techniques (light, fluorescence, or electron microscopy) as well as more recent and developing ones (Scanning Ion Conductance Microscopy and Atomic Force Microscopy) to study the CM morphology and structure is of great importance in cardiopathology and clinical cardiology. The next sections of this review will therefore focus on how these technologies are used to visualize the intra- and extra-cellular structure of the CMs.

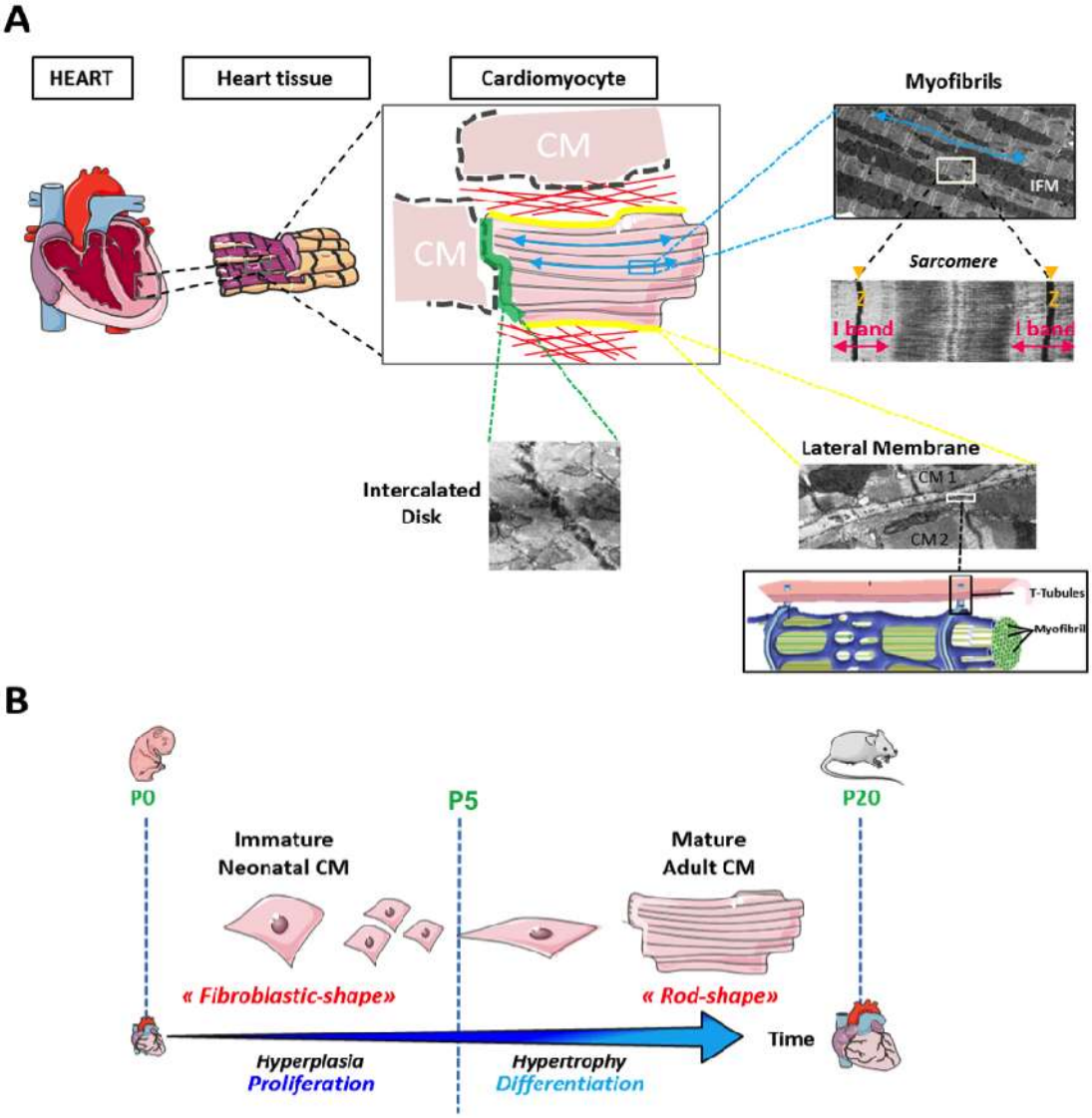

Figure 2. (A) Overview of the cardiomyocyte.CM = cardiomyocyte; Red = Extra Cellular Matrix; Green band = Intercalated Disk; Yellow band = lateral membrane; Blue arrows: Myofibrills; IFM = Interfibrillar Mitochondria; Z= Z-line. Electron microscopy images of some corresponding specialized domains are shown. (B) Cardiomyocyte maturation. CM maturation occurs after birth and duration varies from one species to another, occurring during the first postnatal 20 days (P20) in rodents. The postnatal cardiac maturation is associated with an increase of the cardiac mass and involves two consecutive steps : a 1st step of hyperplasia associated with the neonatal CM proliferation (P0 to P5) followed by the hypertrophy step (P5 to p20) during which CM proliferation stops and the CM increases in size and undergoes a differentiation process leading to the conversion of its fibroblastic-like morphology toits typical mature rod-shape.

3. MICROSCOPY TECHNIQUES USED TO STUDY CARDIOMYOCYTES

Optical microscopy techniques as well as electron microscopy have been now used for several years to visualize the CM structure and organization. More recently, Scanning Ion Conductance Microscopy (SICM) was developed to image the surface of living CMs at high resolution and helped refining the general understanding of the CM structure and function in cardiac diseases. In this section, we will discuss the interest of each type of microscopy for the exploration of CMs.

3.1. Classical microscopy techniques.

3.1.1. Optical microscopy coupled to colorimetric assays.

Given the large size of the CM, it is possible to visualize the cells with standard light microscopy. It allows analyzing

architecture of myocardium and some cellular details with a resolution down to the micrometer scale [9]–[14]. This kind of microscopy is routinely used in pathological diagnosis in clinical context. Although its microscale resolution is too low to distinguish the different organites within the cells, the association of colorimetric methods helps visualizing them. For example, the use of hematoxylin and eosine (HE) stain, the gold standard in pathological diagnosis, allows coloring the cell nucleus in deep-blue and the cell cytoplasm in pink (Figure 3A). This coloration method therefore allows depicting cell's nucleus morphology or architecture defects (wavy CMs), as well as identifying necrotic CMs within a cardiac tissue biopsy [15], a key feature in HF. Colorimetric methods also allows detecting myocardial fibrosis (Masson's trichrome stain), an important factor contributing to the onset of HF, characterized by the increase of collagen fibers within the cardiac tissue [16]. Other staining techniques, not described here, can also be used to detect apoptotic (TUNEL staining) [17] or ischemic CMs (Hematoxylin-basic fuchsin-picric acid) [18]. However, while histomorphology analysis gives the possibility to analyze the different cellular components of the whole cardiac tissue, fluorescence microscopy offers better possibilities to go further into the structure of CMs and of their intracellular components by focusing on the analysis of specific components of the CM.

3.1.2. Optical microscopy coupled to fluorescence.

Compared to visible light microscopy that only allows a global appreciation of the CM morphology, fluorescence microscopy is a useful technique to detect more specific anomalies. Different fluorescent dyes are classically used to study the CM structure; among them, fluorescent wheat-germ agglutinin (WGA) staining helps delineating the CM plasma membrane (Figure 3B; IF microscopy) and thus allows to accurately measure the CM area and quantify CM hypertrophy, a critical HF precursor [19, 20]. Immunofluorescence methods using specific antibodies against different proteins of the CM, and their visualization through a secondary fluorescent antibody are more widespread within the scientific community. For instance, antibodies targeting α-actinin, a cytoskeletal actin-binding protein localized at the Z-line of sarcomeres, are useful to outline the sarcomeres state of CMs (Figure 2A). Immunolocalization of connexin-43, one of the specific components of sarcomeres, can reveal defects in IDs. Another example of fluorescent dyes used to explore the structure/function of CMs is the Di-8-Anepps (ANEP), a fast-response molecule fluorescing in response to electrical potential changes at the CM plasma membrane. Thus, ANEP-fluorescence microscopy allows depicting Ca^{2+} exchanges taking place between sarcolemmal and sarcoplasmic reticulum calcium channels at the T-tubules level and which are necessary for the CM contraction. Thanks to this technique, it is therefore possible, to show the organization of the T-tubules network or its disorganization in cardiac failing conditions [21]. Although fluorescence microscopy brings us a step further into the extra- and intra-cellular architecture of CMs, its resolution does not exceed 200-350 nm and it is thus not suitable to depict macromolecular structures in the nanometer range.

3.2. Electron Microscopy.

Alternative to the optical microscopy is the electron microscopy which principle relies on beams of energetic electrons bombarded over the sample surface and allowing a resolution up to the nanoscale (up to 50 pm at maximum in specific conditions [22]). Electron microscopy can be declined into Transmission Electron Microscopy (TEM) or Scanning Electron Microscopy (SEM), which are two complementary techniques. Indeed, while TEM allows visualizing the ultrastructure of CMs at high resolution, SEM is better suited to study their 3D morphology.

The first type of electron microscopy, TEM, emerged in 1959 thanks to the work of Knoll and Kuger [23]. TEM uses ultra-thin sample sections and beams of electrons that scatter the sample in depth and allows the visualization of the intracellular components organization. To this end, samples are first fixed, embedded in a resin and then cut into 60 to 90 nm sections, which finally undergo different negative staining treatments. Thus, this sample conditioning does not allow working on living cells and TEM observations are always performed on fixed cells. However, TEM-based imaging of a biological sample such as the CM allows visualization of the intracellular organites, such as mitochondria, as well as myofilaments or the lateral membrane structure, with a very high resolution [24] (Figure 3C). Another advantage of such technique is that it can be used on isolated CMs, but also on the whole cardiac tissue, therefore allowing the accurate localization of CMs anomalies with its surrounding tissue environment [25].

Now, although TEM is a powerful technique to visualize CMs ultrastructure at high resolution, it only gives a restricted view from the interior of the CM. Thus, appreciation of the global ultrastructure of the whole CM needs analysis of several successive sample layers, a procedure that is time-consuming. In order to observe the exterior of CMs and to visualize their 3D morphology, SEM is a better suited methodology and provides complementary information to the TEM.

The second type of electron microscopy, SEM, developed in 1938 by von Ardenne [26, 27], allows an observation of samples and of their surface in 3D (Figure 3C). As for TEM, SEM requires CMs samples fixation. Then, a specific solution containing metal ions is vaporized on these samples and finally beamed electrons are scanned all over. In the case of SEM, the detected signals come principally from either the Back-Scattered Electrons (BSE) reflected from the sample's vaporized surface with metal ions, or from the Secondary Electrons (SE) resulting from the interaction of the electron beam with atoms at or near the surface of the sample. Depending on the type of detectors, SE or BSE can be used as signals to produce images of samples surface; in the case of SE, the resolution of images is higher (up to 1 nm [28] instead of 10 with BSE), and in the case of BSE, chemical contrasts on the surface are better detected. Thus, SEM allows an observation of the whole surface of the CM when compared to TEM, and therefore can provide information on their global extracellular morphology. However, the intracellular visualization of the CM is impossible with SEM. To circumvent these problems, an evolution of the SEM combined to a cryofracture method, called cryo-SEM [29], was developed. It consists in cryo-fixing biological samples by plunging them into sub-cooled nitrogen and fracturing them. While still allowing the 3D

observation of CMs similarly to SEM, this method presents the advantage to visualize their intracellular content at the level of the fractures (Figure 3C) [30].

Despite the high resolution and complementarity of SEM and TEM techniques, these methods are still limited by the sample preparation that always requires a fixation step, which can impact the structure of biological samples thus leading to misinterpretations of physiological/pathophysiological cell structures. Today, a novel electron microscopy emerges, the environmental scanning electron microscopy (ESEM) [31]. It is a SEM based technique but the sample can stay in a "wet" environment. ESEM allows observation of live samples, and prevent from fixing. However, there is not yet any study on cardiomyocytes using this instrument. In this context, it is naturally that researchers have evolved toward microscopy techniques allowing the imaging of living CMs such as SICM as developed in the next paragraph.

3.3. SICM to study living cardiomyocytes.

Living CMs structure can be explored through the use of SICM, a near-field microscopy technique [32]. This microscopy method consists in a probe electrically charged with an electrolyte solution, approached to the surface of the sample (which is non-conductive to ions) in an electrolyte bath of the opposite charge. When the tip nears the surface of the sample the ionic conductance decreases, which is reflected by a decrease of the current. These current variations are measured thanks to an amplifier and are used as a feedback to adjust the distance between the tip and the sample. Therefore, the trajectory of the tip follows the ionic heterogeneities of the interface, which allows reconstructing a 3D image of the surface of the sample. This method has been used to observe living CMs [33] at a nanoscale resolution (up to 20 nm) [34], corresponding to the probe size [35]. Recent studies, performed by Gorelik *et al.*, used SICM to visualize the topography of living CMs from healthy and failing hearts [21], [36]. In their first study performed in 2009 [21], the authors showed that the surface of healthy living CMs exhibits a periodic alternation of area more or less conductive to ions (Figure 3D) that is lost in failing hearts and seems to correlate with lower T-tubules density as shown by fluorescent staining. Although this technique presents a great interest for studying living CMs, the deduced topography of the CM surface obtained using SICM is indirect, since the probe and the sample do not physically interact. Thus, the subsequent topography images may not reflect the "true" topography of the sample, but more likely the ionic heterogeneity of the CM interface [37]. Moreover, CMs exhibit a high ionic heterogeneity at their cell surface, making SICM an inappropriate method to study their topography. In this context, AFM, an imaging and a force technology, offers many advantages. It can be operated in liquid, at controlled temperature, on living cells, and can reveal the surface topography by the use of a sharp tip directly interacting with the sample. Moreover, the specific advantage of AFM over SICM relies on the possibility to measure nanomechanical properties of cell membranes and underlying cellular components. In the next section, we will focus on the use of this technique for the study of CMs.

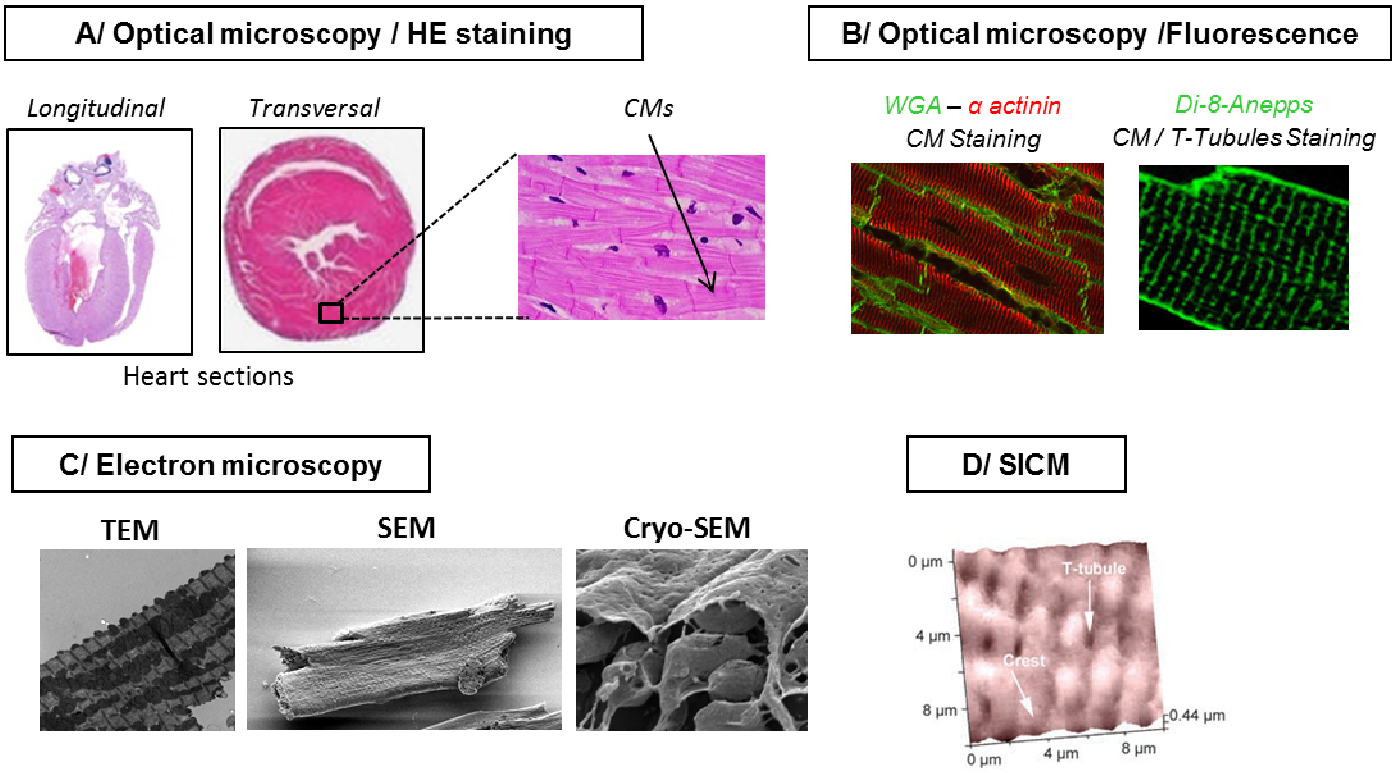

Figure 3. Microscopy techniques for cardiomyocytes imaging. (A) CM morphology and global components organization detected by visible light microscopy coupled with Hematoxylin and Eosine (HE) staining or (B) Fluorescence. (C) Electron microscopy given access to: ultrastructural details of the CM using Transmission Electron microscopy (TEM), CM 3D relief by Scanning Electron Microscopy (SEM) or both ultrastructural and 3D details of the CM by Cryo-SEM. (D) Topography of the lateral membrane of the CM deduced by Scanning Ion-Conductance Microscopy analysis.

4. ATOMIC FORCE MICROSCOPY: FROM THE CM PREPARATION TO THE EXPERIMENT

The AFM invented by Binnig, Quate and Gerber in 1986 [38] has been used in many studies for visualizing biological structures, for measuring the cell's nanomechanical properties, and for studying biological systems at the single cell or the single molecule level [39–44]. This technique belongs to the category of Scanning Probe Microscopy (SPM). The principle of the first SPM was to measure the tunneling current [45] between a sharp tip and a conductive surface [46]. By adjusting the tip position, the current was kept constant and a topographical image was reconstructed. In the case of the AFM, the feedback is not on the tunneling current but on the force applied by the tip on the sample, or on the amplitude/frequency of oscillations on the AFM tip, in vacuum, air or liquid. An AFM is a valuable imaging tool that can be operated in contact mode, in Tapping® mode, or in advanced force curve based modes (like Quantitative Imaging™, from JPK instruments or PeakForce QNM from Bruker [42, 47]). But more than an imaging tool, an AFM is also a force machine able to measure forces in the pN range. In the force spectroscopy mode, forces *versus* distance curves are recorded and give access to the sample nanomechanical and adhesive properties [48–51]. Moreover, the advantage of this microscopy is that acquisitions can be performed in liquid, on living cells. To this end, cells should be immobilized firmly enough in order to withstand lateral frictions induced by the tip while scanning the surface, but without denaturing them [52]. If this point is critical in microbiology, it is usually not a big issue for mammalian cells analysis as they tend to spread on surfaces or can be easily immobilized on matrix proteins coated surfaces (fibronectin, laminin, collagen etc.) [53, 54]. However, in the case of CMs, immobilization of the cells is not the only prerequisite for AFM experiments; CMs are indeed delicate cells that rapidly dedifferentiate when extracted from their physiological environment, and should therefore follow good practice preparation. Sample preparation is therefore a pertinent issue that needs to be carefully addressed; this is the subject of the next section.

4.1. Nature and conditioning of samples for AFM experiments.

Sample conditioning (*i. e.* living or fixed cells) as well as AFM experimental conditions (temperature and CO_2) (Table 1) are key steps in the process of acquiring reliable AFM data. However, the most important parameter that will influence AFM results relies on the nature of the CMs used; CMs obtained from embryonic/neonatal hearts [55], or CMs isolated from adult animals [56] (Table 1). Indeed, CMs coming from adult animals exhibit a differentiated rod-shape with a highly structured plasma membrane, while embryonic cells adopt a fibroblastic-like shape with a less-organized surface. These two CMs types and their purification, as well as the conditioning procedures for AFM experiments will be described in the next paragraphs.

4.1.1. Sample nature: embryonic/neonatal or adult cardiomyocytes.

In 1994, Riehle and coworkers worked on CMs coming from embryos that were 20-30 µm long and 5-10 µm wide, so 7 times smaller than CMs from adult animals [55, 57]. These cells were obtained following extraction from 6 to 9-days-old embryonic hearts directly after cardiac tissue slicing and enzymatic digestion. The extracted cells are then incubated in their culture medium and among them, only CMs will adhere to the culture plastic flask. Finally, after washing away non- adherent cells, the embryonic CMs sample is ready for AFM experiments.

This preparation can be achieved quite easily and AFM acquisition on fibroblastic-like shaped CMs is not limited by the time, as these cells easily proliferate and do not undergo rapid dedifferentiation that can modify their structural surface [55, 58] (Figure 4B).

The procedure used to purify CMs from adult animals is trickier and accordingly, few AFM or SPM studies have been conducted on adult CMs. Basically, adult CMs purification relies on the Langendorff method [59]. In this method, hearts are first extracted from rodents, typically a 2 months-old adult mouse or rat, and are then canulated on the Langendorff system via the aorta, but it is possible to use other animals than mice or rats, such as rabbits and guinea pig. The only differences are the cannula size, the perfusion times and the viability of the myocytes. Hearts are then perfused with different solutions containing different component (such as Na^+, K^+, Hepes, Taurine, butaneidone monoxime (BDM), etc…) in order to increase CMs viability. Each component influence the cells viability as well as the coating of the petri dish (see [61] for a valuable discussion on this subject). Moreover CMs isolation is a tricky question and many researchers are still working to improve the viability of the isolated CMs. These perfused solutions are composed of a washing solution, a decalcifying solution (inhibition of CMs contraction during the procedure) and a specific enzymatic solution allowing detachment of the CMs from the ECM. Following digestion, hearts are dissected and CMs separated by mechanical dissociation. After this step, CMs were separated from the debris by gravity filtration through nylon gauze (with 250µm a mesh), and the CMs sediment can be recuperated (Figure 4A). A supplementary step should be done for the restoration of Ca^{2+} allowing increasing the CMs viability. The CMs are kept alive in MEM solution modified with or without a contractile inhibitor such as BDM or blebbistatine as a function of the measured parameter [61]. Although the isolation of adult CMs needs more practice than for embryonic/neonatal CMs, the use of such adult CMs is more relevant to understand the adult pathologies while the study of embryonic or neonatal cells can lead to misinterpretations. There is thus a major interest in working with adult CMs to understand the adult physio/pathophysiology. In literature, we can found a third procedure: the isolation of adult CMs from human heart[7, 62].

The CMs are extracted from atrial and ventricular tissues those were obtained from patients undergoing corrective cardiac surgery. These hearts pieces were placed in decalcifying solution followed by incubation in enzymatic solution; afterwards the steps are similar to the methods described above.

However, due to their mature state, these cells require that AFM data are acquired quite quickly after their purification (2-3 hours). Indeed, adults rod-shaped CMs are fragile cells, unable to proliferate and that start to spontaneously dedifferentiate into more

fibroblastic-shaped morphology [63] as soon as they are removed from their natural 3D cardiac tissue environment. This dedifferentiation process obliviously impacts the structural organization of the surface of healthy CMs thus needing a rapid examination of these cells. In literature we can found the experiments done on the CMs 6-8 hours and even after 24 hours after extraction[64], after this time, the contractile capacity and the macroscopic morphology are maintained. Therefore, it is possible to use these CMs for experiments such as electrophysiology, but it seems difficult to use CMs for an observation on ultrastructure of cell membrane 6-8 hours after extraction.

It is then clear that the nature of CMs, either it is embryonic/neonatal or adult will lead to different AFM results (Table 1). However, whatever the CMs nature, the cells conditioning can also lead to differences in the AFM results.

Table 1. AFM experiments conditions found in the literature

Nature of CMs	Beating CMs	Conditioning for AFM	AFM mode	T° and CO2	Reference
Chicken embryo CMs	+	Living cells	Mechanosensor	XX	Riehlen*et al.*, 1994
Chicken embryo CMs	+	Living cells	Mechanosensor	37°C, 5% CO2	Domke*et al.*, 1999
Mice adult CMs	-	Living cells	Force Spectroscopy	37°C, 5% CO2	Genet *et al.*, 2012
Rats adult CMs	+	Living cells	Mechanosensor	XX	Liu *et al.*, 2012
Rats adult CMs	+	Living cells	Mechanosensor	XX	Mizutani Y *et al.*, 2012
Rat adult CMs	n/a	Living cells	Force Spectroscopy	RT, no CO2	Sumita Yoshikawa *et al.*, 2013
Mice adult CMs	-	Fixed cells	Force Spectroscopy	RT, no CO2	Benech*et al.*, 2014
Mice adult CMs	-	Living cells	Force Spectroscopy	37°C, 5% CO2	Dague *et al.*, 2014
Rabbit adult CMs	-	Living cells	Force Spectroscopy	XX	Mathur *et al.*, 2001

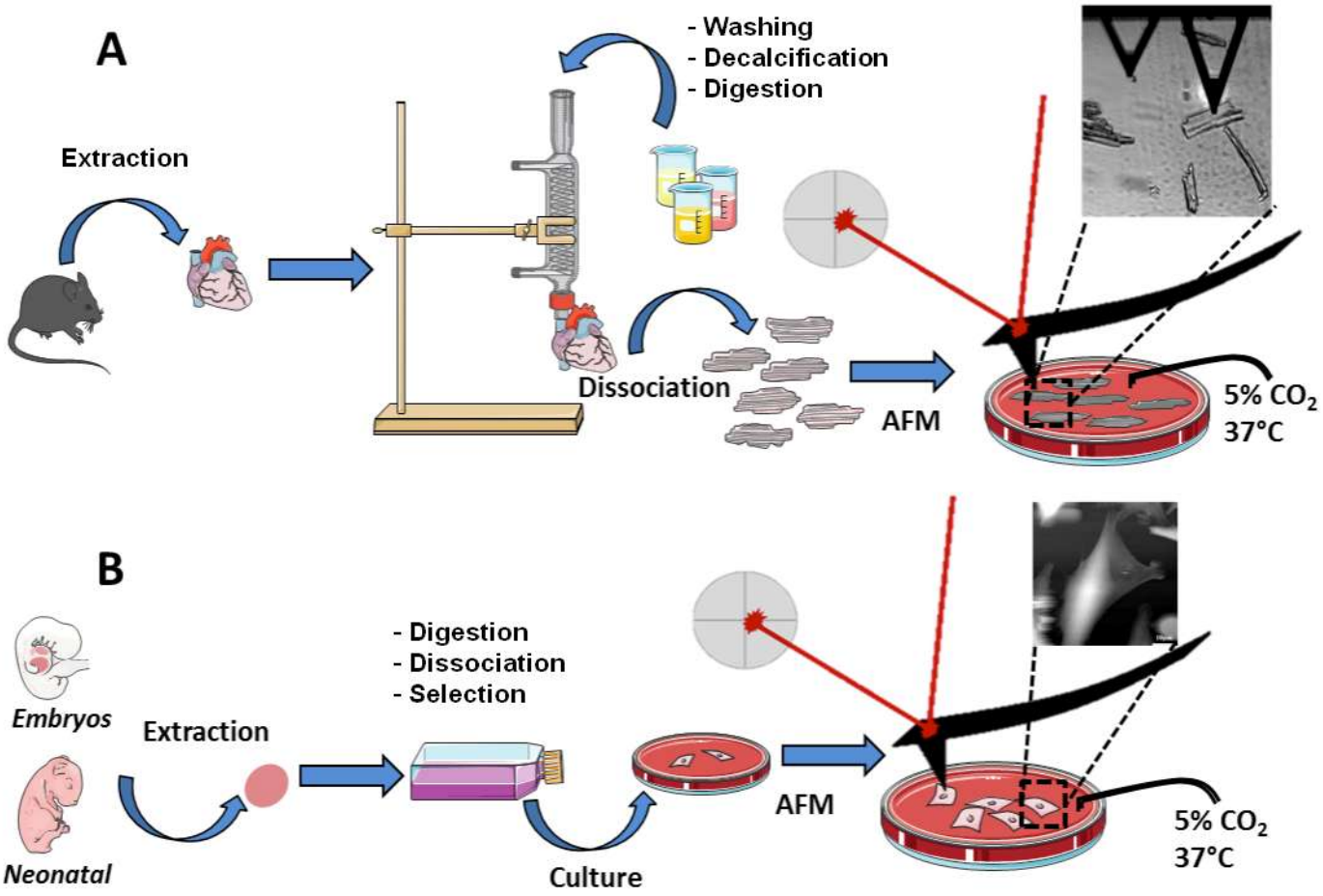

Figure 4. (A) Adult cardiomyocyte purification.Step 1: heart extraction, step 2: heart canulation on a Langerhoff system and washing /digestion with different solutions-step 3: mechanical dissociation, step 4: AFM acquisition on non beating CMs kept alive at 37° C in their cuture medium all along experiment using the perfusing cell; (B) Neonatal/Embyonic cardiomyocyte purification step 1: embryonic heart or neonatal heart extraction, step 2: washing/ digestion with different solutions and direct CMs selection by adhesion to the flask, step 3: Culture during 1-2 days for maturation, step 4: AFM acquisition on beating CMs kept alive at 37° C all along experiment using the perfusing.

4.1.2. Cardiomyocytes conditioning.

Once isolated either from embryos or adults animals, CMs must be immobilized in order to perform AFM experiments. Two different technics are found in the literature; the first one consists in fixing the cells using Paraformaldehyde or Glutaraldehyde [65] (Table 1). In this case, AFM experiments can be performed quite easily as no temperature control, nor CO_2 perfusion will be needed. Another interest of such technic is that experiments are not limited by the time, since fixed cells do not evolve over time. However, no data on the contractility of cells can be generated using this immobilization method. Moreover, fixation procedure can modify the natural structure/morphology of cells.

The second technic consists in the culture of CMs immediately after their isolation in a specific culture medium on laminin-coated plates, a major component of the basement membrane of the adult CM in the cardiac tissue reinforcing their adhesion. Such method can maintain them in living conditions as long as they are cultured at 37°C in 5% CO_2; AFM acquisitions are thus performed in similar conditions in liquid condition and in the presence or not of CM contraction inhibitors (depending on the study purpose) (Table 1). This allows acquiring topographic images or nanomechanical maps of the CMs cell surface [54, 66, 67], as well as evaluating CMs contractility [55, 58, 68, 69].

As already stated above, AFM was originally developed for nanoscale imaging and nanomechanical measurement; the description of imaging modes (paragraph 4.2), force spectroscopy mode (paragraph 4.3) as well as the description of advanced modes (paragraphs 4.4 and 4.5) will be presented in the next paragraphs.

4.2. Imaging samples with Atomic Force Microscopy.

The imaging mode allows obtaining sample's topography using three main modes; contact imaging, Tapping® mode and force spectroscopy mode [70].

4.2.1. Contact imaging.

The principle mode of operation of AFM is called contact mode, where the tip is brought into stable contact with the sample. In this mode, the tip-sample normal force is maintained at a constant value. While scanning the sample, the cantilever undergoes deflections, resulting in displacements of the laser on the photodiode. The variations of the position of the laser are treated, in real time, to reconstruct the topography of the sample. This mode, although used in many studies [71, 72], presents an important limitation for living CMs studies as the lateral forces exerted by the tip deform the surface of the membrane. Indeed, as it can be seen on Figure 5C, the CM topography is distorted by the lateral force, which results it the alteration of the hollow/crests organization of the sarcolemma.

4.2.2. Tapping® mode imaging.

In order to avoid lateral forces exerted by the AFM tip, and to keep a high resolution, AFM can be used in Tapping® or oscillating mode. In this mode, the tip is oscillated near the surface with amplitude of 20 to 100 nm and a frequency close to the cantilevers resonance frequency. In this case, the root-mean-square value of the amplitude is used as the feedback parameter. When the tip is oscillated on a higher surface, its amplitude is then reduced; the variation in the amplitude across the sample is recorded to generate a topographic image. A main advantage of oscillating mode is that lateral forces between the tip and the sample are significantly reduced, which avoids the sample damaging associated with contact-imaging. However, in buffer solutions used in biological studies, where the electrolyte concentration is high, interactions with low-range forces can influence the amplitude of the AFM tip; therefore, the contact between the tip and the sample cannot be avoided, which also leads to deformation of the sample (Figure 5D). Another problem of Tapping® mode is that for oscillating, stiff cantilevers must be used, which is not well suited for experiments on soft and fragile samples such as CMs. Moreover, Tapping® mode, as well as contact mode, is only imaging methods; the third mode, force spectroscopy, gives access to the sample topography, but also to its nanomechanical/adhesive properties.

4.2.3. Height cartography.

In force spectroscopy mode, the AFM probe is repeatedly brought towards the surface and then retracted, which allows producing force curves [53]. Several force curves can be recorded over a matrix of points across the sample (Force Volume mode); by measuring the position of the contact point between the tip and the surface on each curve, a height image of the sample can be reconstructed (Figure 5E). The main advantage of this mode is that there is much information that can be extracted from the force curves. Indeed, the indentation part of the force curve can be analyzed to measure the nanomechanical properties (elasticity, stiffness, next section 4.3) of the sample; the retract part of the force curve gives information on the adhesion between the tip and the surface.

4.3. Probing the nanomechanical and adhesive properties of live cells.

Approach curves can be converted into indentation curves (representing only the deformation of the cell) and fitted to theoretical models. Up to now the Hertz or Sneddon models have been used in a vast majority of articles devoted to the measurement of Young's modulus of cells [72–77]. The Hertz model describes the case of elastic deformation of two perfectly homogeneous smooth bodies touching under load. The Young modulus value obtained provides information on the elasticity of the cell surface and also on its deformation. If the Young modulus value decreases, the deformation of the membrane and of the underlying cellular components (depending on the indentation depth chosen for analysis) is more important, and thus the elasticity is lower. For example, the average Young modulus (YM) value of *E. coli* is in the range of 500 kPa [53], whereas the one of a mammalian cell, such as the living CM [54], is in the range of 20 kPa. This difference in the YM is mainly related to the presence of a cell wall in the case of bacteria. In a different disease condition, such as heart failure, the Young modulus value of CMs increases to 40 kPa [54]. However, the reader must understand that YM values are mainly relative and that absolute comparison is hazardous. Indeed, in other papers, the YM of normal living mammalian cardiomyocytes has been measured in the range 35-43 kPa [78] or around 100 kPa [78]. The experimental conditions

(both for AFM measurements and for CMs conditioning) are never the same between two groups. The applied force is different, the model chosen for the force curve analysis is different, the indentation segment analyzed is different, the method used to determine the contact point is different [79]. As a consequence, the results can hardly be compared and only relative comparison between YM measured in the same conditions are valuable

When retracting the tip from the surface, a retract force curve is recorded and can provide information on the adhesion between the tip and the sample. If the experiment is conducted with a functionalized probe, a chemical or a biochemical adhesion can be recorded (depending on the functionalization). For example, hydrophobic probes can be fabricated by functionalizing the tips with hydrophobic alkanthiol [80, 81]; and single molecule interactions can be recorded by functionalizing the tips with antibodies [82, 83].

Force spectroscopy mode is thus very interesting for the study of CMs, because it provides new information on the cell topography but also on new parameters such as adhesion and elasticity of the cell membrane probed. However, a major drawback of this method is the acquisition time as it is time consuming to record individual force curves according to a matrix of points all over the sample. In order to circumvent this issue, new AFM modes were developed; they are called multiparametric imaging modes.

4.4. Multiparametric imaging modes.

Multiparametric imaging modes are recent operating modes based on force curve acquisition. Theses modes are developed to connect simultaneously all the benefits of the AFM technology: high acquisition speed, nanoscale resolution and investigation of the nanomechanical/adhesive properties of the cells, without altering them. HarmoniX and PeakForce QNM are multiparametric acquisition modes developed by the AFM manufacturer Bruker. HarmoniX mode was first created in order to increase the acquisition speed. It was then replaced by the manufacturers by PeakForce QNM technology where a high number of force curves are acquired at high speed all over the sample. The equivalent mode developed by JPK Instruments is called Quantitative Imaging (QI™) mode, and relies on the same principle, although QI™ offers a longer force curve ramp and a lower z-scan rate, better suited for probing single molecule interactions. Each one of these new advanced acquisition modes have been used for the characterization of numerous cell types, such as eukaryotic cells, yeast or microorganisms [84, 85] and biomolecular systems under physiological conditions. Because multiparametric imaging modes give the opportunity to probe the nanomechanical/adhesive properties of living cell in a short period of time, this technology is more suited for short life sample studies. For example, the topography of CMs is rapidly modified during the dedifferentiation period; indeed, its lateral membrane structure and organization can be altered during long experimental procedure. Therefore, multiparametric imaging modes could allow a rapid analysis of living CMs after their extraction.

4.5. Cantilevers used as nanomechanical sensors.

In heart studies, AFM can also be used differently, by recording the time series of beating heart cells using the constant force mode. In this mode the sample height is adjusted so that the cantilever deflection stays constant, using an electronic feedback loop. Therefore, when the CM contracts, the tip, in contact with its surface, undergoes a deflection that is recorded. Using this method, the frequency of the cell beats as well as their forces can be monitored over time and under certain conditions, such as the addition of a pharmaceutical agent [58]. Such results, combined with data obtained in other AFM modes, can give access to new information and create new paradigms in fundamental questions concerning CMs, and their contractile properties. Altogether, AFM technics bring many possibilities to explore isolated cardiomyocyte in disease conditions or submitted to treatments. Examples of such studies will be described in the next section.

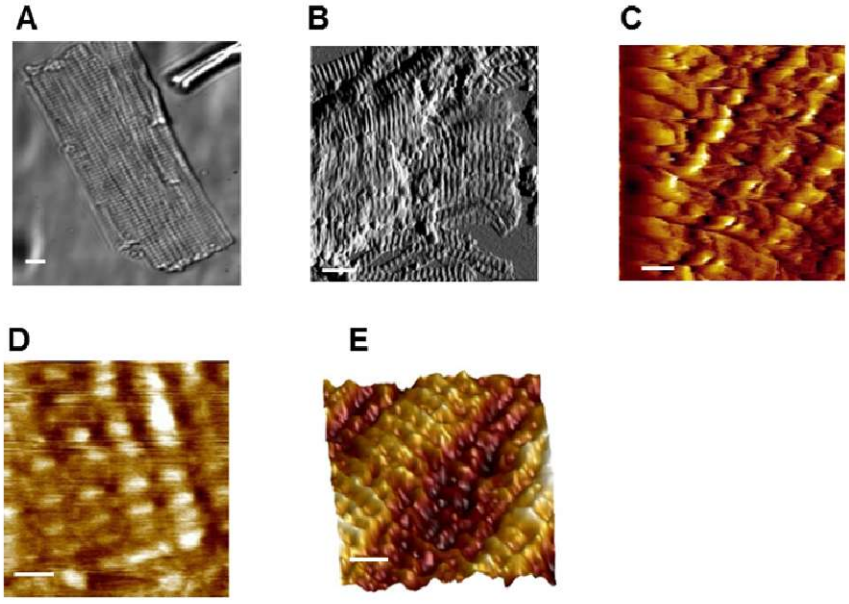

Figure 5. Cell surface topography of living CMs obtained by AFM. CMs were isolated from 2-months old mice hearts **(**A) observation by optical microscopy. Representative images of CMs surface were obtained using: (B) contact mode in liquid on fixed CM, (C) contact mode in liquid on living CM, (D) Tapping mode in liquid on living CM and (E) Force spectroscopy mode in liquid on living CM. Scale bars: 2 µm. Images reprinted from [54].

5. AFM USED TO EXPLORE ISOLATED CARDIOMYOCYTE IN PATHOPHYSIOLOGICAL CONDITIONS

Only few studies in the literature, have studied the CM in physiological condition by AFM [86] and even less have probed the impact of cardiac diseases conditions on CMs using AFM. Among them are studies on HF [54], on diabetes [65], on the effects of an antiarrhythmic on the contraction of CMs [68] and on CMs lacking an essential component of the LM necessary for the stability of their adult rod shape [66].

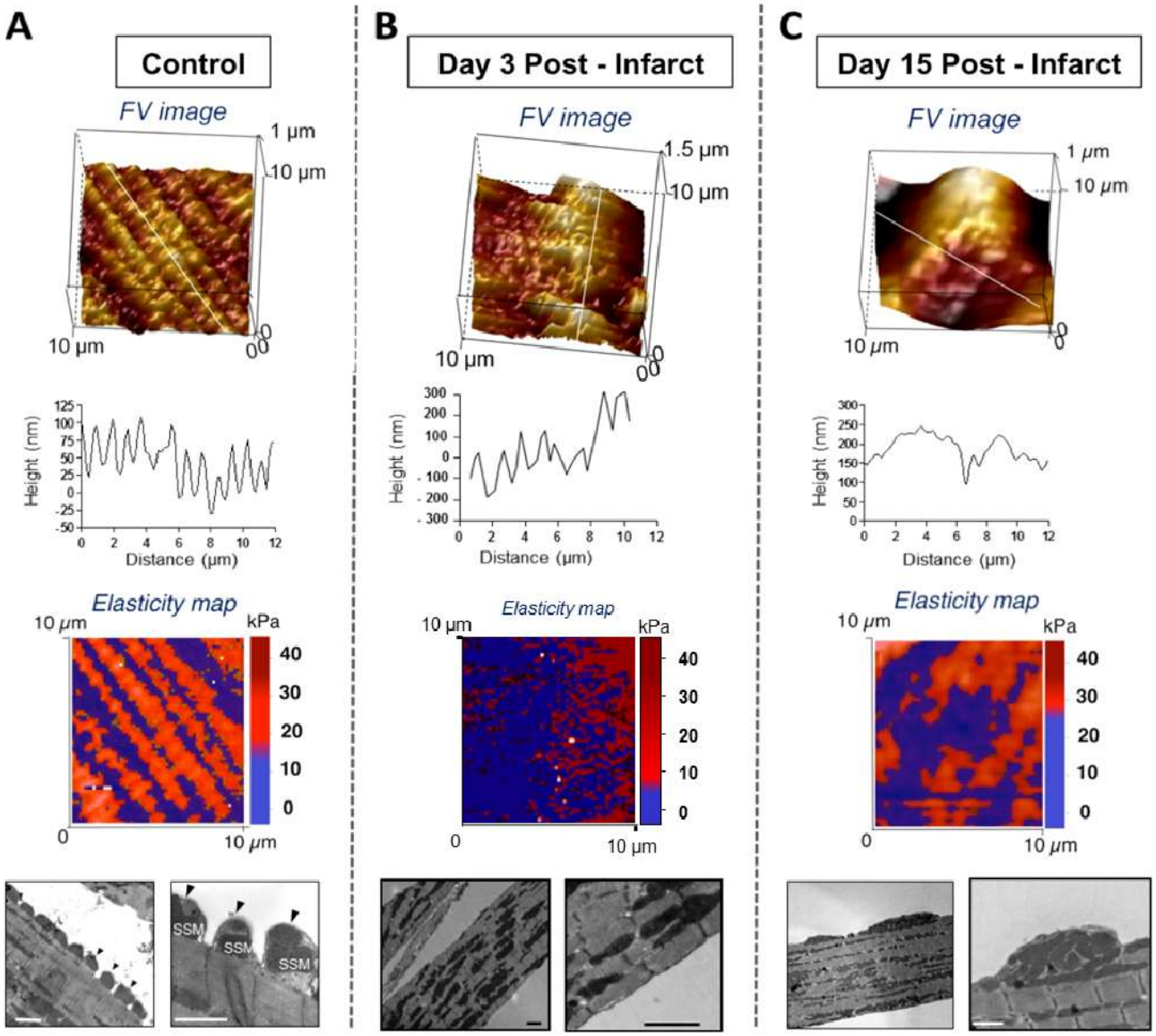

Figure 6. Comparison between topography and biophysical properties of healthy mice CMs and failing CMs. Representative images of a 3D topography (upper panels) and associated elasticity maps of CM surface obtained by AFM force volume (FV) mode analysis. The height variations along the solid line (CM long axis) in FV image are represented in the graphs below. In Elasticity maps from control CM, Young's modulus values ≤ 18 kPa (median value of Young's modulus values measured on the overall CM surface) are depicted in blue while values ≥ 18 kPa are in red. In CMs from 3 and 15 days post-MI failing mice, Young's modulus values ≤ 28 kPa (median value of Young's modulus values measured on the overall CM surface) are depicted in blue while values ≥ 28 kPa are in red. Lower panels represent electron micrograph of isolated CMs in each conditions and showing: periodic organization of crests at the cell surface filled with subsarcolemmal mitochondria (SSM) in control CMs, complete loss of crests and associated SSM in 3 days post-MI CMs, alternation of area with flat surface and mitochondria heaps.. Reprinted from [54].

5.1. AFM used to study living CMs in heart failure.

A recent study by Dague *et al.* [24] showed how AFM can be used to follow the morphological/nanomechanical changes in the LM structure of 2 months-old adult living CMs from failing mice (permanent coronary ligation /experimental infarct model). To this end, non-beating adult CMs isolated and immobilized by laminin were analyzed at 3 (initial IC) and 15 days (advanced IC) post-infarct using force spectroscopy measurements in a controlled atmosphere (37°C, 5% CO_2) with an applied force of 2nN and analyzed with the Hertz model, in order to follow the kinetics of CM structural evolution during HF. In healthy conditions (non-failing mice), the surface topography of the CM presents a highly structured organization with a periodic alternation of crests and hollows (Figure 6A), a feature already observed with SICM at lower resolution [21, 36]. However, compared to SICM, nanomechanical properties (elasticity map) of the surface could also be probed, and indicated that crests were stiffer compared to hollows (Figure 6A). Further TEM and AFM stiffness tomography

(elasticity in-depth in the sample) [51] analysis demonstrated that this increase in stiffness at the crest level, was in fact related to the presence of subsarcolemmal mitochondria (SSM) located beneath the LM. Interestingly, at 3 days post-infarct, the LM of CMs lost their periodic crests/hollows topography and exhibited a flat structure (Figure 6B), correlating with a decreased Young modulus at the surface as well as in depth as shown by force spectroscopy experiments.. TEM observations performed in 3 days post-infarct CMs revealed that the loss of crests and the decreased Young modulus were in fact related to the loss of the SSM population. Fifteen days post-infarct, further modifications of the structure of the LM could be observed; topography/force spectroscopy analysis indicated the presence of new higher stiff heaps (Figure 6C) but presenting a heterogeneous distribution at the CM surface. Correlating TEM images showed that cell surface heaps were formed by the accumulation of interfibrillar mitochondria (IFM), which have migrated from the interior of the CM to the cell surface. Therefore, it appears that the organization of mitochondria populations is responsible for the modifications of the Young modulus of the LM of the CMs probed. This study was the first to combine TEM and AFM observations on living adult CMs and helped to get further insights into the molecular mechanisms underlying HF in mice.

5.2. Use of AFM to study the CMs membrane in diabetes.

Another study by Benech *et al.* [65] focused on the consequences of type 1 diabetes on the nanomechanical properties of CMs. In this work, type 1 diabetes was induced in mice by a single administration of Streptozotocin, a molecule promoting the selective necrosis of pancreatic cells. CMs used for AFM experiments were then purified from primary culture 3 months following the Streptozotocin injection. Imaging acquisition was performed using contact mode on paraformaldehyde fixed CMs ,and individual force curves were recorded using Force spectroscopy mode ("Point and Shoot") on top of the adult CMs isolated and plated on polylysine. This method allowed the authors to measure an increase of the stiffness of the cell membrane of diabetic CMs, compared to healthy CMs. A particular interest of this study is the combined analysis by confocal microscopy, which made possible to explore the cytoskeleton simultaneously. Thus, diabetic CMs have been shown to harbor a diffuse and irregular actin organization, compared to healthy cells that present well-defined and ordered actin filaments. The authors then concluded that the cytoskeleton disorganization could be responsible for the increase in stiffness of the CMs cell surface.

5.3. Using AFM to probe the role of ephrin-B1 in the cardiomyocyte architecture.

In another recent study conducted by Genet *et al*. [66], AFM was used to explore the role of ephrin-B1, a transmembrane protein localized at the LM of adult CMs. Combining different fluorescence and electron microscopy imaging together with *in vivo* experiments, the authors of this study demonstrated that this protein plays a key role in the stabilization of the adult CM rod-shape, thus allowing the cohesion of the cardiac tissue. To support their conclusions, AFM was used as a complementary method to study non-beating living CMs purified from 2-3 months old mice deleted or not for the gene encoding for ephrin-B1 protein (*efnb1*$^{-/-}$ Knock-out KO), to probe the elasticity of the LM of CMs. Force spectroscopy experiments performed on adult isolated CMs, immobilized on laminin coated dishes in a controlled atmosphere (37°C with 5% CO_2) with an applied force limited to 2nN and analyzed with Hertz model, have shown that the absence of ephrin-B1 impacted the elasticity of the CM lateral membrane, with a 3-fold increase of the Young modulus in CMs isolated from *efnb1* KO mice compared to control CMs (Figure 7A).

5.4. Probing the effects of ibutilide on the heart contraction using AFM.

Finally in a study conducted by Liu *et al.* [68], the authors did not use AFM as an imaging tool nor as a force machine, but as a nanomechanical sensor. This strategy, used for the first time by Radmacher *et al.* in 1994 [87], allowed the authors to monitor the cell's beats frequency and force, as presented in Figure 7B, in the absence or presence of ibutilide, an antiarrhythmic agent indicated for atrial fibrillation and dysfunction of the sinus rhythm. The results obtained by the authors demonstrated that this molecule induced a decrease in the contraction force, and an increase in the beating frequency (from 0.59 Hz to 0.83 Hz). The authors could thus conclude that ibutilide could prevent ventricular arrhythmias by decreasing the contraction force of the CMs. This opens new perspectives for using AFM as a tool to screen for molecules efficiency potentially useful for the treatment of cardiac pathologies.

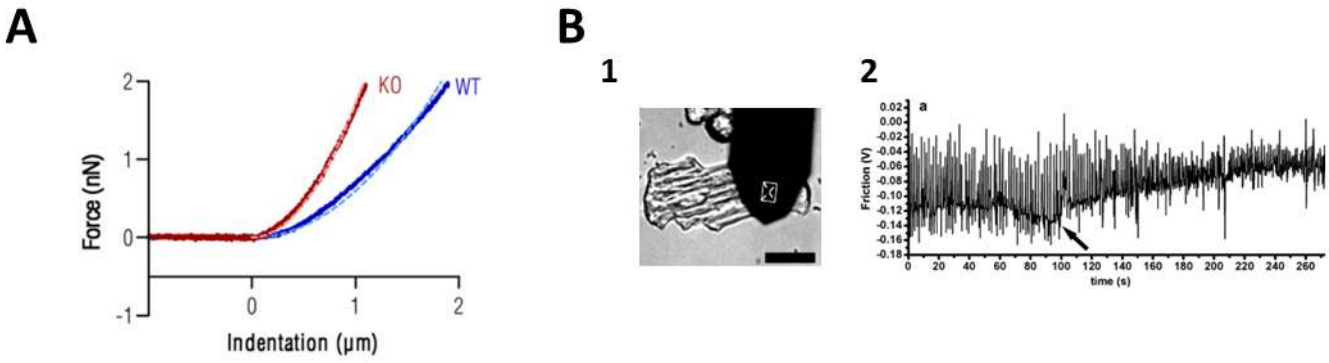

Figure 7. (A) Ephrin B1 stabilizes the stiffness of the CM. Representative single indentation curve (*plain line*) from AFM studies performed on wild type (*blue*) or KO (*red*) Eprin B1 living CMs. In both cases, the Hertz Model (*dotted line*) fitted quite well with experiment. (B) The cantilever torsional force is used to measure the CM contractions (1). Record of a CM contractions performed by a system based on the cantilever sensitivity, before and after (arrow) the addition of an arrythmic agent (2).

6. CONCLUSIONS

These recent years AFM nanotechnology has evolved into a multifunctional tool that opens new possibilities for studying CMs from a different angle. Combining this technology with preexisting microscopies imaging (confocal, fluorescence, TEM/SEM), has allowed generating new information on the structure of the membrane of CMs, as well as on their nanomechanical properties. AFM technics using the cantilever as a mechanosensor also provided a useful tool for studying the contraction of these cells. However, the number of research articles using AFM still remains very low, and we present here the first review dedicated to its use in cardiology. There are therefore many open possibilities to explore this field and AFM studies should be extensively applied to many different cardiac pathophysiological states to explore modifications of the surface of the CM. The recent advances proposed by AFM manufacturers, such as multiparametric imaging modes will allow acquiring data on living cells in a reasonable time, and at high resolution. This way studies performed on living cells will be easier to perform, and therefore the fundamental knowledge generated on cells close to their physiological conditions will increase. Multiparametric imaging will also be of great use to probe the adhesive properties of the cardiomyocytes; this has never been explored, and combining this approach with AFM tips functionalization strategies with biomolecules will bring valuable results to the field. Indeed, using this method, mapping of specific proteins at the surface of cardiomyocytes in different conditions or submitted to treatments will be possible. This way the knowledge on the functions and roles of specific protein (such as ephrins) will be deciphered. Altogether, developing existing AFM approaches and using advanced techniques such as multiparametric imaging with functionalized AFM tips is of great interest in a field such as cardiology. The molecular architecture of cardiomyocytes can be probed using these technics, and, combined with electronic or optical microscopies giving access to the "inside" of cells, light will be shed on the mechanisms underlying public-health pathologies, such as heart failure and other heart diseases.

7. REFERENCES

[1] D. Lloyd-Jones, R. J. Adams, T. M. Brown, M. Carnethon, S. Dai, G. De Simone, T. B. Ferguson, E. Ford, K. Furie, C. Gillespie, A. Go, K. Greenlund, N. Haase, S. Hailpern, P. M. Ho, V. Howard, B. Kissela, S. Kittner, D. Lackland, L. Lisabeth, A. Marelli, M. M. McDermott, J. Meigs, D. Mozaffarian, M. Mussolino, G. Nichol, V. L. Roger, W. Rosamond, R. Sacco, P. Sorlie, V. L. Roger, R. Stafford, T. Thom, S. Wasserthiel-Smoller, N. D. Wong, J. Wylie-Rosett, Heart disease and stroke statistics--2010 update: a report from the American Heart Association , *Circulation*, 121, 7, e46‑e215, **2010**.

[2] A. L. Bui, T. B. Horwich, G. C. Fonarow, Epidemiology and risk profile of heart failure , *Nat. Rev. Cardiol.*,. 8, 1, 30‑41, **2011**.

[3] G. S. Francis, Pathophysiology of chronic heart failure , *Am. J. Med.*, 110, 7, Suppl. 1, 37‑46, **2001**.

[4] J. A. Hill, E. N. Olson, Cardiac plasticity , *N. Engl. J. Med.*, 358, 13, 1370‑1380, **2008**.

[5] Gallo P,d'Amati G., Cardiomyopathies, In : Silver MD, Gotlieb Al, Schoen FJ, editors. *Cardiovascular pathology*, Chapter 10, **2001**.

[6] A. K. Biala, L. A. Kirshenbaum, The interplay between cell death signaling pathways in the heart , *Trends in Cardiovascular Medicine*, **2014**.

[7] M. Leu, E. Ehler, J. C. Perriard, Characterisation of postnatal growth of the murine heart , *Anat. Embryol. (Berl.)*, 204, 3, 217‑224, **2001**.

[8] D. V. Miller, M. P. Revelo Diagnostic Pathology: Cardiovascular, Published by Amirsys®, **2014**.

[9] Y.-Y. Zhou, S.-Q. Wang, W.-Z. Zhu, A. Chruscinski, B. K. Kobilka, B. Ziman, S. Wang, E. G. Lakatta, H. Cheng, et R.-P. Xiao, Culture and adenoviral infection of adult mouse cardiac myocytes: methods for cellular genetic physiology , *Am. J. Physiol. - Heart Circ. Physiol.*, 279, 1, H429‑H436, **2000**.

[10] C. F. Deschepper, S. Picard, G. Thibault, R. Touyz, et J.-L. Rouleau, Characterization of myocardium, isolated cardiomyocytes, and blood pressure in WKHA and WKY rats , *Am. J. Physiol. - Heart Circ. Physiol.*, 282, 1, H149‑H155, **2002**.

[11] M. Zheng, R. Hou, et R.-P. Xiao, Acidosis-induced p38 MAPK activation and its implication in regulation of cardiac contractility, *Acta Pharmacol. Sin.*, 25, 10, 1299‑1305, **2004**.

[12] H. K. Saini et N. S. Dhalla, Defective calcium handling in cardiomyocytes isolated from hearts subjected to ischemia-reperfusion, *Am. J. Physiol. Heart Circ. Physiol.*, 288, 5, H2260‑2270, **2005**.

[13] Z. Kabaeva, M. Zhao, et D. E. Michele, Blebbistatin extends culture life of adult mouse cardiac myocytes and allows efficient and stable transgene expression , *Am. J. Physiol. Heart Circ. Physiol.*, 294, 4, H1667‑1674, **2008**.

[14] A. Gartner, T. Pereira, R. Gomes, A. Lucia, M. Lacueva, S. Geuna, P. Armada-da-Silva, et A. Colette, Mesenchymal Stem Cells from Extra-Embryonic Tissues for Tissue Engineering – Regeneration of the Peripheral Nerve , in *Advances in Biomaterials Science and Biomedical Applications*, R. Pignatello, Éd. InTech, **2013**.

[15] A. Cohen, Coeur et médecine interne, published by De Boeck Secundair, **2002.**

[16] B. Maisch, E. Bauer, G. Hufnagel, et R. Rohkamm, The use of endomyocardial biopsy in heart failure , *Eur. Heart J.*, 9, suppl H, 59‑71, **1988**.

[17] A. Saraste, K. Pulkki, M. Kallajoki, P. Heikkilä, P. Laine, S. Mattila, M. S. Nieminen, M. Parvinen, et L. M. Voipio-Pulkki, Cardiomyocyte apoptosis and progression of heart failure to transplantation, *Eur. J. Clin. Invest.*, 29, 5, 380‑386, **1999**.

[18] J. Rajs, Histological diagsis of myocardial injury. Comparison of hematoxylin-basic fuchsin-picric acid (HBFP)-stained sections obtained during autopsy with isolated viable rat cardiac myocytes exposed to anoxia, *Acta Pathol. Microbiol. Scand. [A]*, 87A, 4, 289‑297, **1979**.

[19] S. Jovanovic, A. J. Grantham, J. E. Tarara, J. C. Burnett, A. Jovanovic, et A. Terzic, Increased number of cardiomyocytes in cross-sections from tachycardia-induced cardiomyopathic hearts., *Int. J. Mol. Med.*, **1999**.

[20] O. R. Coelho-Filho, R. V. Shah, R. Mitchell, T. G. Neilan, H. Moreno, B. Simonson, R. Kwong, A. Rosenzweig, S. Das, et M. Jerosch-Herold, Quantification of Cardiomyocyte Hypertrophy by Cardiac Magnetic Resonance Implications for Early Cardiac Remodeling, *Circulation*, 128, 11, 1225‑1233, **2013**.

[21] A. R. Lyon, K. T. MacLeod, Y. Zhang, E. Garcia, G. K. Kanda, M. J. Lab, Y. E. Korchev, S. E. Harding, et J. Gorelik, Loss of T-tubules and other changes to surface topography in ventricular myocytes from failing human and rat heart, *Proc. Natl. Acad. Sci.*, 106, 16, 6854‑6859, **2009**.

[22] H. Sawada, F. Hosokawa, T. Kaneyama, T. Tomita, Y. Kondo, T. Tanaka, Y. Oshima, Y. Tanishiro, N. Yamamoto, et K. Takayanagi, Performance of R005 Microscope and Aberration Correction System, in *EMC 2008 14th European Microscopy Congress 1–5 September 2008, Aachen, Germany*, M. Luysberg, K. Tillmann, et T. Weirich, Éd. Springer Berlin Heidelberg, 47‑48, **2008**.

[23] M. Knoll et J. Kugler, Subjective Light Pattern Spectroscopy in the Encephalographic Frequency Range, *Nature*, 184, 4701, 1823‑1824, **1959**.

[24] E. Dague, G. Genet, V. Lachaize, C. Guilbeau-Frugier, J. Fauconnier, C. Mias, B. Payré, L. Chopinet, D. Alsteens, S. Kasas, C. Severac, J. Thireau, C. Heymes, B. Honton, A. Lacampagne, A. Pathak, J.-M. Sénard, et C. Galés, Atomic force and electron microscopic-based study of sarcolemmal surface of living cardiomyocytes unveils

unexpected mitochondrial shift in heart failure, *J. Mol. Cell. Cardiol.*, 74, 162‑172, **2014**.
[25] D. Chang, Z. Wen, Y. Wang, W. Cai, M. Wani, C. Paul, T. Okano, R. W. Millard, et Y. Wang, Ultrastructural Features of Ischemic Tissue following Application of a Bio-Membrane Based Progenitor Cardiomyocyte Patch for Myocardial Infarction Repair, *PLoS ONE*, 9, 10, **2014**.
[26] D. MacMullan, Von Ardenne and the scanning electron microscope, *Proc. R. Microsc. Soc.*, 23, 283‑288, **1988**.
[27] M. von Ardenne, Die durch Elektronenstreuung im Objekt verursachten Abbildungsfehler des Elektronenmikroskops und ihr Verhältnis zueinander, *Z. Für Phys.*, 111, 3‑4, 152‑157, **1938.**
[28] F. J. Doucet, L. Maguire, et J. R. Lead, Assessment of cross-flow filtration for the size fractionation of freshwater colloids and particles, *Talanta*, 67, 1, 144‑154, **2005**.
[29] M. Adrian, J. Dubochet, J. Lepault, et A. W. McDowall, Cryo-electron microscopy of viruses, *Nature*, 308, 5954, 32‑36, **1984**.
[30] J. P. Jung, J. M. Squirrell, G. E. Lyons, K. W. Eliceiri, et B. M. Ogle, Imaging cardiac extracellular matrices: a blueprint for regeneration, *Trends Biotechnol.*, 30, 4, 233‑240, **2012**.
[31] A. Bogner, P.-H. Jouneau, G. Thollet, D. Basset, et C. Gauthier, A history of scanning electron microscopy developments: Towards "wet-STEM" imaging, *Micron*, 38, 4, 390‑401, **2007**.
[32] P. Hansma, B. Drake, O. Marti, S. Gould, et C. Prater, The scanning ion-conductance microscope, *Science*, 243, 4891, 641‑643, **1989**.
[33] S. Bergner, P. Vatsyayan, et F.-M. Matysik, Recent advances in high resolution scanning electrochemical microscopy of living cells – A review, *Anal. Chim. Acta*, 775, 1‑13, **2013**.
[34] P. Novak, C. Li, A. I. Shevchuk, R. Stepanyan, M. Caldwell, S. Hughes, T. G. Smart, J. Gorelik, V. P. Ostanin, M. J. Lab, G. W. J. Moss, G. I. Frolenkov, D. Klenerman, et Y. E. Korchev, Nanoscale live-cell imaging using hopping probe ion conductance microscopy, *Nat. Methods*, 6, 4, 279‑281, **2009**.
[35] M. Caldwell, S. J. L. Del Linz, T. G. Smart, et G. W. J. Moss, Method for Estimating the Tip Geometry of Scanning Ion Conductance Microscope Pipets, *Anal. Chem.*, 84, 21, 8980‑8984, **2012**.
[36] V. O. Nikolaev, A. Moshkov, A. R. Lyon, M. Miragoli, P. Novak, H. Paur, M. J. Lohse, Y. E. Korchev, S. E. Harding, et J. Gorelik, β2-Adrenergic Receptor Redistribution in Heart Failure Changes cAMP Compartmentation, *Science*, 327, 5973, 1653‑1657, **2010**.
[37] M. Miragoli, A. Moshkov, P. Novak, A. Shevchuk, V. O. Nikolaev, I. El-Hamamsy, C. M. F. Potter, P. Wright, S. H. S. A. Kadir, A. R. Lyon, J. A. Mitchell, A. H. Chester, D. Klenerman, M. J. Lab, Y. E. Korchev, S. E. Harding, et J. Gorelik, Scanning ion conductance microscopy: a convergent high-resolution technology for multi-parametric analysis of living cardiovascular cells, *J. R. Soc. Interface R. Soc.*, 8, 60, 913‑925, **2011**.
[38] S. M. Evans, D. Yelon, F. L. Conlon, et M. L. Kirby, Myocardial Lineage Development, *Circ. Res.*, 107, 12, 1428‑1444, **2010**.
[39] Y. F. Dufrêne, Application of atomic force microscopy to microbial surfaces: from reconstituted cell surface layers to living cells, *Micron Oxf. Engl. 1993*, 32, 2, 153‑165, **2001**.
[40] D. J. Müller et Y. F. Dufrêne, Atomic force microscopy: a nanoscopic window on the cell surface, *Trends Cell Biol.*, 21, 8, 461‑469, **2011**.
[41] J. J. Heinisch, P. N. Lipke, A. Beaussart, S. El Kirat Chatel, V. Dupres, D. Alsteens, et Y. F. Dufrêne, Atomic force microscopy - looking at mechanosensors on the cell surface, *J. Cell Sci.*, 125, 18, 4189‑4195, **2012**.
[42] Y. F. Dufrêne, D. Martínez-Martín, I. Medalsy, D. Alsteens, et D. J. Müller, Multiparametric imaging of biological systems by force-distance curve-based AFM, *Nat. Methods*, 10, 9, 847‑854, **2013**.
[43] Y. F. Dufrêne et A. E. Pelling, Force nanoscopy of cell mechanics and cell adhesion, *Nanoscale*, 5, 10, 4094‑4104, **2013**.
[44] P. J. de Pablo et M. Carrión-Vázquez, Imaging biological samples with atomic force microscopy, *Cold Spring Harb. Protoc.*, 2014, 2, 167‑177, **2014**.
[45] G. Binnig, H. Rohrer, C. Gerber, et E. Weibel, Tunneling through a controllable vacuum gap, *Appl Phys Lett*, 40, 2, 178‑180, **1982**.
[46] P. K. Hansma, V. B. Elings, O. Marti, et C. E. Bracker, Scanning tunneling microscopy and atomic force microscopy: application to biology and technology, *Science*, 242, 4876, 209‑216, **1988**.
[47] D. Alsteens, V. Dupres, S. Yunus, J.-P. Latgé, J. J. Heinisch, et Y. F. Dufrêne, High-Resolution Imaging of Chemical and Biological Sites on Living Cells Using Peak Force Tapping Atomic Force Microscopy, *Langmuir*, 28, 49, 16738‑16744, **2012**.
[48] W. F. Heinz et J. H. Hoh, Spatially resolved force spectroscopy of biological surfaces using the atomic force microscope, *Trends Biotechnol.*, 17, 4, 143‑150, **1999**.
[49] G. Longo, L. M. Rio, C. Roduit, A. Trampuz, A. Bizzini, G. Dietler, et S. Kasas, Force volume and stiffness tomography investigation on the dynamics of stiff material under bacterial membranes, *J. Mol. Recognit.*, 25, 5, 278‑284, **2012**.
[50] C. Roduit, S. Sekatski, G. Dietler, S. Catsicas, F. Lafont, et S. Kasas, Stiffness tomography by atomic force microscopy, *Biophys. J.*, 97, 2, 674‑677, **2009**.
[51] C. Roduit, B. Saha, L. Alonso-Sarduy, A. Volterra, G. Dietler, et S. Kasas, OpenFovea: open-source AFM data processing software, *Nat. Methods*, 9, 8, 774‑775, **2012**.
[52] K. El Kirat, I. Burton, V. Dupres, et Y. F. Dufrene, Sample preparation procedures for biological atomic force microscopy, *J. Microsc.*, 218, 3, 199‑207, **2005**.
[53] L. Chopinet, C. Formosa, M. P. Rols, R. E. Duval, et E. Dague, Imaging living cells surface and quantifying its properties at high resolution using AFM in QI^{TM} mode, *Micron*, 48, 26‑33, **2013**.
[54] E. Dague, G. Genet, V. Lachaize, C. Guilbeau-Frugier, J. Fauconnier, C. Mias, B. Payré, L. Chopinet, D. Alsteens, S. Kasas, C. Severac, J. Thireau, C. Heymes, B. Honton, A. Lacampagne, A. Pathak, J.-M. Sénard, et C. Galés, Atomic force and electron microscopic-based study of sarcolemmal surface of living cardiomyocytes unveils unexpected mitochondrial shift in heart failure, *J. Mol. Cell. Cardiol.*, 74, 162‑172, **2014**.
[55] M. Riehle et J. Bereiter-Hahn, Ouabain and digitoxin as modulators of chick embryo cardiomyocyte energy metabolism, *Arzneimittelforschung.*, 44, 8, 943‑947, **1994**.
[56] M. J. Masse et I. Harary, Primary cultures of embryonic rat heart cells, *In Vitro*, 17, 5, 388‑392, **1981**.
[57] M. C. Denyer, M. Riehle, S. T. Britland, et A. Offenhauser, Preliminary study on the suitability of a pharmacological bio-assay based on cardiac myocytes cultured over microfabricated microelectrode arrays, *Med. Biol. Eng. Comput.*, 36, 5, 638‑644, **1998**.
[58] J. Domke, W. J. Parak, M. George, H. E. Gaub, et M. Radmacher, Mapping the mechanical pulse of single cardiomyocytes with the atomic force microscope, *Eur. Biophys. J. EBJ*, 28, 3, 179‑186, **1999**.
[59] K. J. Broadley, The Langendorff heart preparation—Reappraisal of its role as a research and teaching model for coronary vasoactive drugs, *J. Pharmacol. Methods*, 2, 2, 143‑156, **1979**.
[60] K. Broadley, The Langendorff heart preparation—Reappraisal of its role as a research and teaching model for coronary vasoactive drugs, *J. Pharmacol. Methods*, 2, 2, 143‑156, **1979**.
[61] W. E. Louch, K. A. Sheehan, et B. M. Wolska, Methods in Cardiomyocyte Isolation, Culture, and Gene Transfer, *J. Mol. Cell. Cardiol.*, 51, 3, 288‑298, **2011**.
[62] J. O. Bustamante, T. Watanabe, D. A. Murphy, et T. F. McDonald, Isolation of single atrial and ventricular cells from the human heart., *Can. Med. Assoc. J.*, 126, 7, 791‑793, **1982**.
[63] J. Gorelik, L. Q. Yang, Y. Zhang, M. Lab, Y. Korchev, et S. E. Harding, A novel Z-groove index characterizing myocardial surface structure, *Cardiovasc. Res.*, 72, 3, 422‑429, **2006**.
[64] Y.-Y. Zhou, S.-Q. Wang, W.-Z. Zhu, A. Chruscinski, B. K. Kobilka, B. Ziman, S. Wang, E. G. Lakatta, H. Cheng, et R.-P. Xiao, Culture and adenoviral infection of adult mouse cardiac myocytes: methods for cellular genetic physiology, *Am. J. Physiol. - Heart Circ. Physiol.*, 279, 1, H429‑H436, **2000**.
[65] J. C. Benech, N. Benech, A. I. Zambrana, I. Rauschert, V. Bervejillo, N. Oddone, et J. P. Damián, Diabetes increases stiffness of live cardiomyocytes measured by atomic force microscopy nanoindentation, *Am. J. Physiol. Cell Physiol.*, ajpcell.00192.2013, **2014**.
[66] G. Genet, C. Guilbeau-Frugier, B. Honton, E. Dague, M. D. Schneider, C. Coatrieux, D. Calise, C. Cardin, C. Nieto, B. Payré, C.

Dubroca, P. Marck, C. Heymes, A. Dubrac, D. Arvanitis, F. Despas, M.-F. Altié, M.-H. Seguelas, M.-B. Delisle, A. Davy, J.-M. Sénard, A. Pathak, et C. Galés, Ephrin-B1 is a novel specific component of the lateral membrane of the cardiomyocyte and is essential for the stability of cardiac tissue architecture cohesion, *Circ. Res.*, 110, 5, 688‑700, **2012**.

[67] W. Sumita Yoshikawa, K. Nakamura, D. Miura, J. Shimizu, K. Hashimoto, N. Kataoka, H. Toyota, H. Okuyama, T. Miyoshi, H. Morita, K. Fukushima Kusano, T. Matsuo, M. Takaki, F. Kajiya, N. Yagi, T. Ohe, et H. Ito, Increased passive stiffness of cardiomyocytes in the transverse direction and residual actin and myosin cross-bridge formation in hypertrophied rat hearts induced by chronic β-adrenergic stimulation, *Circ. J. Off. J. Jpn. Circ. Soc.*, 77, 3, 741‑748, **2013**.

[68] Y. Liu, J. Feng, L. Shi, R. Niu, Q. Sun, H. Liu, J. Li, J. Guo, J. Zhu, et D. Han, In situ mechanical analysis of cardiomyocytes at nano scales, *Nanoscale*, 4, 1, 99‑102, **2012**.

[69] Y. Mizutani, K. Kawahara, et T. Okajima, Effect of isoproterenol on local contractile behaviors of rat cardiomyocytes measured by atomic force microscopy, *Curr. Pharm. Biotechnol.*, 13, 14, 2599‑2603, **2012**.

[70] F. Pillet, L. Chopinet, C. Formosa, et É. Dague, Atomic Force Microscopy and pharmacology: From microbiology to cancerology, *Biochim. Biophys. Acta BBA - Gen. Subj.*, 1840, 3, 1028‑1050, **2014**.

[71] E. Dague, D. Alsteens, J.-P. Latgé, et Y. F. Dufrêne, High-Resolution Cell Surface Dynamics of Germinating Aspergillus fumigatus Conidia, *Biophys. J.*, 94, 2, 656‑660, **2008**.

[72] C. Formosa, M. Grare, E. Jauvert, A. Coutable, J. B. Regnouf-de-Vains, M. Mourer, R. E. Duval, et E. Dague, Nanoscale analysis of the effects of antibiotics and CX1 on a Pseudomonas aeruginosa multidrug-resistant strain, *Sci Rep*, 2, **2012**.

[73] C. Formosa, M. Grare, R. E. Duval, et E. Dague, Nanoscale effects of antibiotics on P. aeruginosa, *Nanomedicine Nanotechnol. Biol. Med.*, 8, 1, 12‑16, **2012**.

[74] C. Formosa, M. Schiavone, H. Martin-Yken, J. M. François, R. E. Duval, et E. Dague, Nanoscale Effects of Caspofungin against Two Yeast Species, Saccharomyces cerevisiae and Candida albicans, *Antimicrob. Agents Chemother.*, 57, 8, 3498‑3506, **2013**.

[75] F. Pillet, S. Lemonier, M. Schiavone, C. Formosa, H. Martin-Yken, J. M. Francois, et E. Dague, Uncovering by Atomic Force Microscopy of an original circular structure at the yeast cell surface in response to heat shock, *BMC Biol.*, 12, 1, 6, **2014**.

[76] L. Chopinet, C. Roduit, M.-P. Rols, et E. Dague, Destabilization induced by electropermeabilization analyzed by atomic force microscopy, *Biochim. Biophys. Acta*, 1828, 9, 2223‑2229, **2013**.

[77] A. Cerf, J.-C. Cau, C. Vieu, et E. Dague, Nanomechanical Properties of Dead or Alive Single-Patterned Bacteria, *Langmuir*, 25, 10, 5731‑5736, **2009**.

[78] A. B. Mathur, A. M. Collinsworth, W. M. Reichert, W. E. Kraus, et G. A. Truskey, Endothelial, cardiac muscle and skeletal muscle exhibit different viscous and elastic properties as determined by atomic force microscopy, *J. Biomech.*, 34, 12, 1545‑1553, **2001**.

[79] H.-J. Butt, B. Cappella, et M. Kappl, Force measurements with the atomic force microscope: Technique, interpretation and applications, *Surf. Sci. Rep.*, 59, 1‑6, 1‑152, **2005**.

[80] E. Dague, D. Alsteens, J. P. Latge, C. Verbelen, D. Raze, A. R. Baulard, et Y. F. Dufrêne, Chemical force microscopy of single live cells, *Nano Lett*, 7, 10, 3026‑3030, **2007**.

[81] D. Alsteens, E. Dague, P. G. Rouxhet, A. R. Baulard, et Y. F. Dufrene, Direct measurement of hydrophobic forces on cell surfaces using AFM, *Langmuir*, 23, 24, 11977‑11979, **2007**.

[82] P. Hinterdorfer et Y. F. Dufrêne, Detection and localization of single molecular recognition events using atomic force microscopy, *Nat. Methods*, 3, 5, 347‑355, **2006**.

[83] E. Jauvert, E. Dague, M. Severac, L. Ressier, A. M. Caminade, J. P. Majoral, et E. Trévisiol, Probing single molecule interactions by AFM using bio-functionalized dendritips, *Sens. Actuators B Chem.*, 168, 436‑441, **2012**.

[84] C. Formosa, M. Schiavone, A. Boisrame, M. L. Richard, R. E. Duval, et E. Dague, Multiparametric imaging of adhesive nanodomains at the surface of Candida albicans by atomic force microscopy, *Nanomedicine Nanotechnol. Biol. Med.*, **2014**.

[85] D. Alsteens, H. Trabelsi, P. Soumillion, et Y. F. Dufrêne, Multiparametric atomic force microscopy imaging of single bacteriophages extruding from living bacteria, *Nat. Commun.*, 4, 2926, **2013**.

[86] S. C. Lieber, N. Aubry, J. Pain, G. Diaz, S.-J. Kim, et S. F. Vatner, Aging increases stiffness of cardiac myocytes measured by atomic force microscopy nanoindentation, *Am. J. Physiol. - Heart Circ. Physiol.*, 287, 2, H645‑H651, **2004**.

[87] M. Radmacher, J. P. Cleveland, M. Fritz, H. G. Hansma, et P. K. Hansma, Mapping interaction forces with the atomic force microscope, *Biophys. J.*, 66, 6, 2159‑2165, **1994**.

8. ACKNOWLEDGEMENTS

VL holds a PhD grant from Federative University of Toulouse Midi-Pyrénées and Region Midi-Pyrénées, CF and GS are postdoctoral researchers respectively at LAAS-CNRS and ITAV-CNRS. ED is a scientific researcher at CNRS, CG is a scientific researcher at INSERM. This research is supported by FRM, Grant # ING 21040129094.

© 2015 by the authors. This article is an open access article distributed under the terms and conditions of the Creative Commons Attribution license (http://creativecommons.org/licenses/by/4.0/).